High resolution double-resonance spectroscopy on Rydberg states of CO

Marcel Drabbels, Johannes Heinze,[a] J. J. ter Meulen, and W. Leo Meerts
Department of Molecular and Laser Physics, University of Nijmegen, Toernooiveld, 6525 ED Nijmegen, The Netherlands

(Received 1 February 1993; accepted 29 June 1993)

The Rydberg states $L\ ^1\Pi(v=0)$, $L'\ ^1\Pi(v=1)$, $K\ ^1\Sigma^+(v=0)$, $W\ ^1\Pi(v=0)$, and $W'\ ^1\Pi(v=2)$ have been studied in a 2+1 double-resonance detection scheme with a resolution of 0.005 cm^{-1}. Accurate molecular constants have been derived for these states. From the observed linewidths of individual rotational transitions, predissociation rates for the Rydberg states have been deduced. For the first time a clear J and e/f dependence for the predissociation of CO has been observed. One of the states causing the observed predissociation could be identified as the $D'\ ^1\Sigma^+$ state.

I. INTRODUCTION

Carbon monoxide is believed to be the most abundant interstellar molecule after H_2 and it's isotopic variants. It is therefore an important tracer for H_2, which in most cases cannot be detected directly in interstellar clouds, circumstellar envelopes, and in planetary and cometary atmospheres. The ratio abundance of CO to that of H_2 is difficult to determine from observations but can be derived by complex theoretical models.[1] One of the most important but also one of the most uncertain parameters in these models is the photodissociation rate of CO in the wavelength range between 91.2 nm, the absorption continuum of atomic hydrogen, and 111.8 nm corresponding to the dissociation limit of CO.[2]

Some years ago Letzelter *et al.*[3] recorded the absorption spectrum in this wavelength range and derived photoabsorption cross sections and predissociation rates. As an important result it was established that the XUV photodissociation of CO takes place rather via discrete line absorption than via continuous absorption. Since then many experiments have been performed to determine accurate photoabsorption cross sections,[4–6] line positions and photodissociation rates for the electronic states in the XUV region. Employing a 10 m VUV spectrograph Eidelsberg *et al.*[7–10] performed the most extensive study on CO in the region between 91.2 and 115.2 nm. Most of the observed electronic states could be assigned to members of Rydberg series converging to the $X\ ^2\Pi$ and $A\ ^2\Pi$ states in the CO^+ ion and molecular constants for the four most important isotopes of CO were obtained. Recently Levelt *et al.*[11,12] accurately determined the absolute line positions for most of the Rydberg states observed by Eidelsberg *et al.* using a laser based XUV spectrometer calibrated to the I_2 standard. In addition to direct XUV absorption spectroscopy, other detection schemes can be applied. Optogalvanic spectroscopy has been applied to study inter-Rydberg transitions in CO.[13–16] Accurate molecular constants for the involved Rydberg states were obtained. Furthermore, different resonantly enhanced multiphoton ionization[17–19] (REMPI) and four-wave mixing schemes[20,21] have been applied to study the Rydberg states of CO.

In this paper we present a high resolution study on five Rydberg states in the energy range between 102 300 and 103 500 cm^{-1}, i.e., the $L\ 4p\pi\ ^1\Pi(v=0)$, $L'\ 3d\pi\ ^1\Pi(v=1)$ and $K\ 4p\sigma\ ^1\Sigma^+(v=0)$ states all converging to the electronic ground state of CO^+, the $W\ (A\ ^2\Pi)\ 3s\sigma\ ^1\Pi(v=0)$ state converging to the first electronically excited state $A\ ^2\Pi$ of CO^+ and the $W'\ ^1\Pi(v=2)$ which is most probably a valence state. Besides molecular constants also predissociation rates for the different electronic states are determined.

The method used here to study the Rydberg states of CO is similar to the method used by Klopotek and Vidal[22] who after populating a single rotational level in the $A\ ^1\Pi$ state of CO probed the $E\ ^1\Pi$ state with a second laser. The detection scheme we used to study Rydberg states in carbon monoxide is given in Fig. 1. In a first step the CO molecules are two photon excited from the ground state $X\ ^1\Sigma^+(v=0)$ to a single rotational level in the $B\ ^1\Sigma^+(v=0)$ state. The B state can be populated either via $\Delta J=0$ or via $\Delta J=\pm 2$ transitions, which are however 2–3 orders of magnitude weaker than the $\Delta J=0$ transitions. The population of the B state is monitored by detecting the strong fluorescence from the $B\ ^1\Sigma^+$ to the $A\ ^1\Pi$ state. In the second step the molecules are further excited by a second (probe) laser from the B state to a higher lying Rydberg state. A transition to a Rydberg state causes a depletion of the B state and can therefore be detected by a decrease of the $B \rightarrow A$ fluorescence. By scanning the probe laser a laser-depleted fluorescence dip spectrum of the inter Rydberg transition is obtained. Employing a Fourier limited pulsed laser system for the second step, accurate linewidth measurements can be performed yielding accurate predissociation rates for the Rydberg states.

II. EXPERIMENT

A schematic overview of the experimental setup is given in Fig. 2. Two different laser systems are used in the experiments. Either laser system can be used as the pump laser or the probe laser and are both simultaneously pumped by a Q-switched Nd:YAG laser (Quantel YG 681C-10). The third harmonic of the Nd:YAG laser with

[a]Present address: Deutsche Forschungsanstalt für Luft- und Raumfahrt, Forschungszentrum Stuttgart, W-7000 Stuttgart 80, Germany.

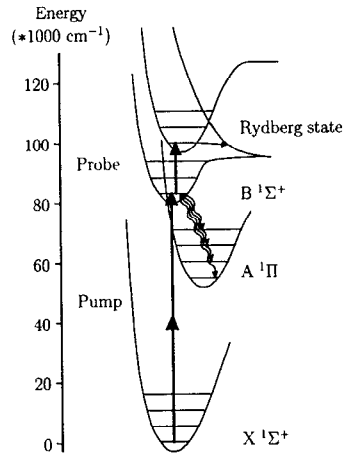

FIG. 1. Detection scheme used to study low-lying Rydberg states of CO.

a pulse energy of 200 mJ is used to pump the laser system which induces the $B \leftarrow X$ transition. The second harmonic of the Nd:YAG laser, pulse energy about 300 mJ, is used to pump the probe laser. One laser system is a commercial pulsed dye laser (Continuum TDL60). When used as pump laser the dye laser is operated on Coumarine 460 dye. The output of the laser is frequency doubled in a BBO crystal to yield 3 mJ of radiation at 230 nm. When used as probe laser the laser operates on DCM dye yielding 60 mJ of tunable light between 605–655 nm with a bandwidth of 0.1 cm^{-1}. The absolute frequency of the dye laser is measured with a calibrated monochromator and can be determined within 0.5 cm^{-1}. Relative frequency measurements are performed by recording the transmission fringes of a Fabry-Perot interferometer with a free spectral range of 0.6634 ± 0.0002 cm^{-1}.

The other laser system is a pulsed dye amplifier (PDA) system. When used as pump laser the output of a single frequency ring dye laser (Spectra Physics 380 D), operating on Stilbene 3 dye, is amplified by a four stage PDA system, operating on Coumarine 460. In this way radiation with a bandwidth of 220 MHz and a pulse energy of 10 mJ is obtained. After frequency doubling in a BBO crystal radiation around 230 nm is obtained with a pulse energy of about 1 mJ. When used as probe laser the system is operated on DCM dye. The bandwidth of the amplified laser beam is in this case 135 MHz, whereas the pulse energy is typically 50 mJ. The fact that the bandwidth of the system is smaller when operated in the red than when operated in the blue is caused by the fact that the pulse length of the second harmonic of the Nd:YAG laser is somewhat longer than that of the third harmonic. For absolute frequency measurements the I_2 or Te_2 absorption spectrum[23–25] is recorded simultaneously along with the excitation or fluorescence dip spectrum. For relative frequency calibration the transmission peaks of a pressure and temperature stabilized interferometer with a free spectral range of 299.84 ± 0.05 MHz are recorded.

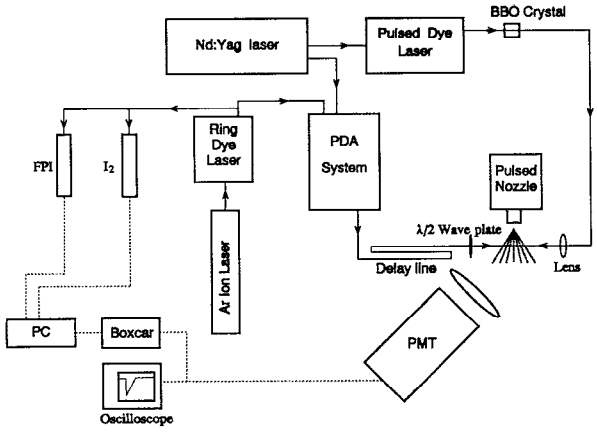

FIG. 2. Schematic overview of the experimental setup.

A molecular jet is formed by expanding 2 atm. neat CO into a vacuum chamber through an electromagnetic pulsed valve with an orifice of 1 mm operating at 10 Hz. The molecular jet is 50 mm downstream of the nozzle crossed by the two counterpropagating laser beams. The pump laser is softly focused by a lens ($f=500$ mm) into the jet in order to excite the CO molecules to a single rotational level in the $B\,^1\Sigma^+(v=0)$ state. The fluorescence from $B\,^1\Sigma^+(v=0) \rightarrow A\,^1\Pi$ is collected by a quartz lens system and imaged onto a photomultiplier. In order to reduce the scattered light a Schott KV 370 glass filter is placed in front of the photomultiplier. The fluorescence signal is processed by a digital oscilloscope (LeCroy 7400) and two boxcar integrators (SRS 250) interfaced with a Personal Computer. The probe laser with a diameter of 2 mm counterpropagates the pump laser and is delayed 10 ns with respect to the pump laser by a delay line of 3 m. The fluorescence during the first few nanoseconds, which is proportional to the initial population of the B state, is used to normalize the fluorescence detected after the probe laser is fired. By introducing a delay between the pump and probe laser coherence effects such as, for example, Autler–Townes splitting[26] are avoided. When the molecules are excited to the B state only some specific M components of a rotational level are populated, due to the selection rules. The fraction of molecules in this rotational level that can be excited to a Rydberg state depends therefore strongly on the polarization of the probe laser. In order to be able to excite all the molecules the polarization of the probe laser can be adjusted by a $\lambda/2$ wave plate.

III. DETERMINATION OF PREDISSOCIATION RATES

The predissociation rate of a Rydberg state is determined by measuring the width of the transition from the $B\,^1\Sigma^+(v=0)$ to this Rydberg state. Assuming that the radiative decay rates for both the B state and the Rydberg state are much smaller than the predissociation rate of the Rydberg state the predissociation rate is given by

$$k_p = 2\pi\Gamma, \tag{1}$$

where Γ is the linewidth (FWHM) of the transition observed. The corresponding lifetime of this state is given by

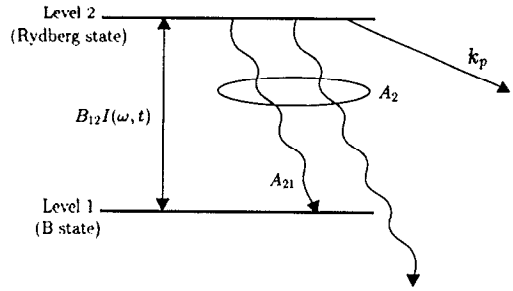

FIG. 3. The two level scheme used to calculate line broadening effects. A_1 is the total radiative decay rate of the B state, A_2 the total radiative decay rate of the Rydberg state, A_{21} the decay rate from the Rydberg state to the B state, B_{12} the usual line integrated Einstein coefficient, $I(t,\omega)$ the laser intensity, and k_p is the predissociation rate of the Rydberg state.

$$\tau=\frac{1}{k_p}=\frac{1}{2\pi\Gamma}. \tag{2}$$

The linewidths observed in the present experiment are, however, not only determined by predissociation but also by the linewidth of the probe laser. The laser has a Gaussian line shape and the line profile observed will therefore be a Voigt profile. It has been shown[27] that the Lorentzian linewidth, in this case caused by the predissociation, is related to the observed linewidth by

$$\Delta\nu_L=\Delta\nu_{\text{obs}}-\frac{(\Delta\nu_G)^2}{\Delta\nu_{\text{obs}}}, \tag{3}$$

where $\Delta\nu_L$, $\Delta\nu_G$, and $\Delta\nu_{\text{obs}}$ are the Lorentzian, Gaussian, and observed linewidth, respectively. In our case the linewidth of the probe laser is much smaller than the observed linewidth and the Lorentzian linewidth is therefore almost equal to the observed linewidth.

In the present experiment a transition to a Rydberg state is observed by a depletion of the intermediate $B\,^1\Sigma^+$ state. However, if a large fraction of the CO molecules in this intermediate state is excited to a Rydberg state the width of the transition will increase due to saturation broadening. In order to determine the effect of saturation broadening on the linewidth we performed calculations on a two-level scheme. Since in our case the predissociation rate of the upper level is much larger than the excitation rate, rate equations can be used instead of the optical Bloch equations.[28] We start with the assumption that the experiment can be described by a two-level scheme as indicated in Fig. 3, thus neglecting the extra loss channel introduced by ionization after absorbing one more photon of the probe laser. Although the ionization rate cannot be exactly determined, since the ionization cross sections of the Rydberg states involved are not known, it can be estimated from the ground state ionization cross section[29] and the laser intensity used (5×10^5 W/cm^2) to be 2 orders of magnitude smaller than the radiative decay rate and excitation rate, justifying the previously made assumption. In the calculations we furthermore assume that at time $t=0$ the B state is instantaneously populated by the pump laser. The rate equations describing the temporal behavior of the populations in the different levels are given by

$$\frac{dN_1}{dt}=-B_{12}I(t,\omega)G(\omega)\left(N_1-\frac{g_1}{g_2}N_2\right)-A_1N_1+A_{21}N_2, \tag{4}$$

$$\frac{dN_2}{dt}=B_{12}I(t,\omega)G(\omega)\left(N_1-\frac{g_1}{g_2}N_2\right)-(A_2+k_p)N_2. \tag{5}$$

Here N_1 and N_2 are the time dependent population in the $B\,^1\Sigma^+$ and Rydberg state, respectively, and g_1 and g_2 the degeneracy of the two states involved. A_1 is the total radiative decay rate of the B state, A_2 the total radiative decay rate of the Rydberg state, A_{21} the decay rate from the Rydberg state to the B state, B_{12} the usual line integrated Einstein coefficient, $G(\omega)$ a Lorentzian line shape function, k_p the predissociation rate of the Rydberg state, and $I(t,\omega)$ the laser intensity of the probe laser. For the laser intensity a Gaussian time profile with a maximum intensity at $t=10$ ns and a width of 5 ns is assumed. The term $B_{12}I(t,\omega)G(\omega)$ is then given by

$$B_{12}I(t,\omega)G(\omega)=\frac{k_p}{(\omega-\omega_0)^2+k_p^2}B_{12}I_0e^{-(10-t)^2/(5/2\sqrt{\ln 2})^2}. \tag{6}$$

Here ω is the laser frequency and ω_0 is the center frequency of the transition.

These rate equations are solved numerically as a function of the laser frequency. In these calculations a value of 3.3×10^7 s^{-1} is used for A_1, corresponding to a lifetime of 30 ns for the B state (see Sec. IV A). The values for A_2 and A_{21} are, however, not known. For A_2 we assumed a value of 1×10^8 s^{-1}. This value corresponds to a lifetime of 10 ns for the Rydberg state, a value common for low lying Rydberg states in CO. For A_{21} a value of 1×10^6 s^{-1} is assumed and for B_{12} a value of 1×10^{11} J^{-1} s^{-1} cm^2. To simulate the experiment where the $B\rightarrow A$ fluorescence is monitored by a boxcar integrator with its gate set 20 ns after the pump laser the quantity describing this fluorescence, A_1N_1, is integrated for times greater than 20 ns. From the resulting calculated line shape the width and the depth of the fluorescence dip are determined. This procedure has been performed for different laser intensities. The results obtained hardly depend on the values for A_{21} and A_2 but vary strongly with the predissociation rate k_p. Figure 4 shows the extra broadening due to saturation of the transition as a function of the depletion of the B state for different values of the predissociation rate. The broadening due to saturation is larger for small values of k_p and becomes independent of k_p for values $k_p\geqslant2.0\times10^{10}$ s^{-1}. For a depletion smaller than 40% the variation in power broadening is smaller than 5% for values of k_p greater than 1.0×10^9 s^{-1}. This variation is well within the experimental error at which the linewidth can be determined (see Sec. IV). In the experiment performed the laser power of the probe laser is kept low so that the depletion of the B state

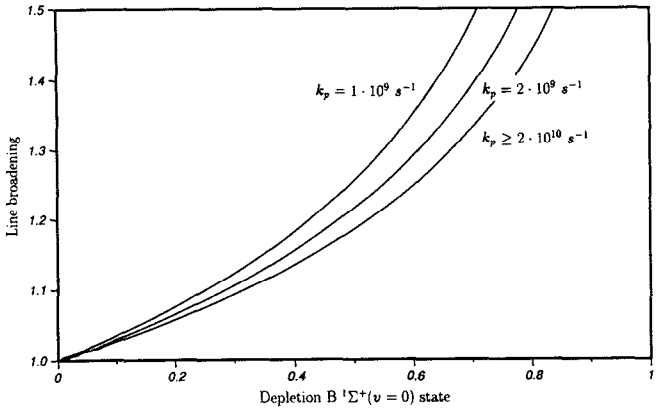

FIG. 4. Calculated line broadening as a function of the depletion of the B state for different predissociation rates, k_p, of the upper state.

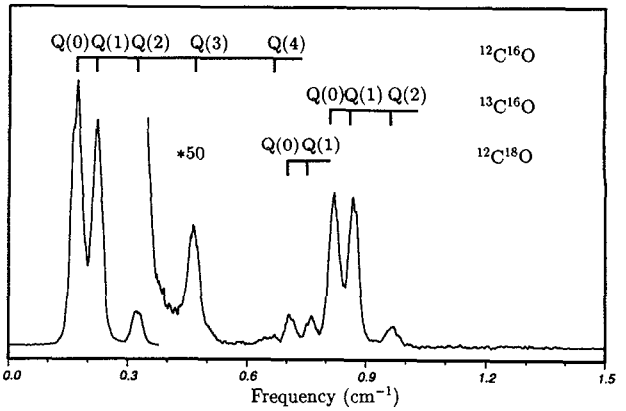

FIG. 5. Excitation spectrum of the $B\,^1\Sigma^+(v=0) \leftarrow X\,^1\Sigma^+(v=0)$ transition around 86 916 cm^{-1}.

is always smaller than 40%. In this case the correction for the saturation broadening can be assumed to be independent of the predissociation rate k_p.

IV. RESULTS

A. $B\,^1\Sigma^+$ state

The $B\,^1\Sigma^+$ state is the first member of the nso Rydberg series converging to the electronic ground state of the carbon monoxide ion. It has been studied extensively in both absorption[7,30] and emission.[7,31] Eidelsberg *et al.*[7] concluded that the $B\,^1\Sigma^+$ state is perturbed by another nearby lying state which causes high rotational and vibrational levels in the B state to predissociate. The $B\,^1\Sigma^+ \leftarrow X\,^1\Sigma^+$ transition has also been studied using 2 photon spectroscopy.[32,33] In this case only Q and O and S branches can be observed. Due to the fact that the potential of the B state is similar to that of the ground state the difference in the rotational constants is very small. As a consequence, the Q branch, at least for low J, cannot be resolved with a normal pulsed dye laser. The O and S transitions can easily be resolved but their intensity is 2–3 orders of magnitude lower than that of the Q branch. With the high power laser systems now available they can be observed.[33]

The two photon excitation spectrum of the $B\,^1\Sigma^+(v=0) \leftarrow X\,^1\Sigma^+(v=0)$ transition is shown in Fig. 5. As can be seen in Fig. 5, the Q branch can just be resolved with our resolution of 780 MHz, which is solely determined by the bandwidth of the laser system. Due to the low rotational temperature of 4 K only the lowest 5 rotational levels can be observed. This makes it possible to observe also transitions of the $^{13}C^{16}O$ and $^{12}C^{18}O$ isotopic species in natural abundance. The $B\,^1\Sigma^+(v=1) \leftarrow X\,^1\Sigma^+(v=0)$ is much weaker due to the Franck–Condon factor and therefore only the Q branch could be observed. The rotational constant in the $v=1$ is so close to that one of the ground state that the Q branch could not be resolved. The observed transitions together with their assignments are listed in Table I.

The observed line frequencies have been fit to the following expression for a $^1\Sigma^+ \leftrightarrow {}^1\Sigma^+$ transition:

$$\nu = T_v + B'_v J'(J'+1) - D'_v J'^2 (J'+1)^2 - [B''_0 J''(J''+1) - D''_0 J''^2 (J''+1)^2]. \quad (7)$$

Here B'_v, D'_v, J' and B''_0, D''_0, J'' refer to the upper and ground states, respectively. The rotational constants for the ground state were kept fixed in the fit at the values obtained by Guelachvili *et al.*[34] The centrifugal distortion constants, D'_v, for the B state were fixed at the values derived by Eidelsberg.[7] The resulting rotational constants for the B state are given in Table II. The agreement between our results and those of Eidelsberg *et al.*[7] are excellent, with one exception however, the value of T_0 for the $^{12}C^{18}O$ isotopomer.

The radiative lifetimes for the vibrational levels in the B state have been measured in many different ways. There is, however, a rather large spread in the values found for the lifetimes. This is caused by the fact that in most of the

TABLE I. Observed and calculated line positions (in cm^{-1}) of the $B\,^1\Sigma^+(v') \leftarrow X\,^1\Sigma^+(v''=0)$ transition for different isotopic species of CO.

Isotope	Transition	Obs. freq.	Obs.-calc.
$^{12}C^{16}O$	$Q(0)$	86 916.149(3)	−0.001
($v'=0$)	$Q(1)$	86 916.204(3)	0.002
	$Q(2)$	86 916.306(3)	0.001
	$Q(3)$	86 916.458(3)	0.002
	$Q(4)$	86 916.652(9)	−0.012
	$S(0)$	86 927.839(3)	0.001
	$S(1)$	86 935.682(3)	0.001
$^{12}C^{16}O$	$Q(0)$	88 998.32(3)	−0.001
($v'=1$)	$Q(1)$	88 998.32(3)	0.001
	$Q(2)$	88 998.32(3)	0.003
$^{13}C^{16}O$	$Q(0)$	86 916.812(3)	−0.001
($v'=0$)	$Q(1)$	86 916.863(3)	0.001
	$Q(2)$	86 916.960(3)	−0.001
$^{12}C^{18}O$	$Q(0)$	86 916.706(3)	−0.001
($v'=0$)	$Q(1)$	86 916.756(3)	0.001

TABLE II. Molecular constants for the $B\,^1\Sigma^+$ state of different isotopic species of CO.

		B' (cm^{-1})	D' (cm^{-1})	T_v (cm^{-1})	τ (ns)
$^{12}C^{16}O$	$v'=0$	1.948 16(23)	6.8×10^{-6} [a]	86 916.1501(19)	29.3(1.6)
	$v'=1$	1.921 902[a]	7.4×10^{-6} [a]	88 998.32(3)	19.8(1.3)
$^{13}C^{16}O$	$v'=0$	1.862 74(44)	6.2×10^{-6} [a]	86 916.8110(19)	29.6(1.6)
$^{12}C^{18}O$	$v'=0$	1.855 53[a]	6.2×10^{-6} [a]	86 916.7047(9)	29.2(1.6)

[a]Kept fixed in the fit at the value obtained by Eidelsberg *et al.* (Ref. 7).

experiments fluorescence trapping and cascading effects play an important role. In our experiment no cascading effects can occur since only one rotational level in the B state is excited and only the $B\rightarrow A$ fluorescence is detected. Fluorescence trapping can, however, occur but by diluting the CO fraction in Ar down to 1% this effect can be avoided. The lifetimes for the different isotopes of CO have been measured on several rotational lines. The values found are listed in Table II and are equal for the different isotopic species. The lifetime for the $B(v=1)$ state is measured to be shorter than that for the $B(v=0)$ state by almost a factor of 1.5. The *ab initio* calculations of Cooper and Langhof[35] and Kirby and Cooper[36] on the B state show a similar effect for the lifetimes of the two vibrational levels. They pointed out that this effect is caused by a strong dependence of the transition moment on the internuclear distance.

B. $L(4p\pi)^1\Pi(v=0)$ state

The L state is a member of the $np\pi$ Rydberg series converging to the ionic ground state $X\,^2\Sigma^+$ of CO^+. It has been studied by direct XUV absorption spectroscopy[8,10,12] and by optogalvanic spectroscopy via the $L\,^1\Pi(v=0)\leftarrow B^1\Sigma^+(v=0)$ transition.[13,14] From these measurements it is known that the L state interacts with another state which causes an accidental perturbation of the $J=7$ level of the $\Pi^-(f)$ component.

The L state is measured using the pulsed dye laser as pump laser to populate one specific rotational level in the B state via an S transition. The PDA system is then used to probe the L state. The observed line frequencies for the $L^1\Pi(v=0)\leftarrow B^1\Sigma^+$ transitions together with their assignments are listed in Table III. The observed line frequencies have been fit to the following expressions for a $^1\Pi\leftarrow{}^1\Sigma^+$ transition:

TABLE III. Observed and calculated line frequencies and the observed linewidths, all in cm^{-1}, of the $L\,^1\Pi(v'=0)\leftarrow B\,^1\Sigma^+(v''=0)$ transition.

Transition	Obs. freq.	Obs.-calc.	Γ
$P(2)$	16 347.913(6)	−0.003	0.023(2)
$P(3)$	16 344.157(6)	0.003	0.047(6)
$Q(2)$	16 355.712(6)	0.002	0.0096(13)
$Q(3)$	16 355.779(6)	0.002	0.0098(11)
$R(2)$	16 367.691(16)	−0.002	0.088(8)
$R(3)$	16 371.884(32)	0.012	0.188(14)

$$\nu_{\Pi^+}=\nu_0+B'_eJ'(J'+1)-D'J'^2(J'+1)^2-[B''J''(J''+1)-D''J''^2(J''+1)^2], \quad (8)$$

$$\nu_{\Pi^-}=\nu_0+B'_fJ'(J'+1)-D'J'^2(J'+1)^2-[B''J''(J''+1)-D''J''^2(J''+1)^2]. \quad (9)$$

Here expression (8) describes transitions to the $\Pi^+(e)$ Λ doublet component probed by P and R transitions and expression (9) transitions to the $\Pi^-(f)$ Λ doublet component probed by Q transitions. It is assumed that the centrifugal distortion constant D' is equal for both Λ doublet components. The rotational constants for the B state were kept fixed in the fit at the values given in Table II. The resulting molecular constants for the L state are given in Table IV together with the constants found in Refs. 8, 10, 12, 13, and 14. The Λ doubling parameter q_π is given by the relation

$$q_\pi=|B'_e-B'_f|. \quad (10)$$

The constant T_0 for the L state can be calculated by adding the value of T_0 of the B state to that of the ν_{00} for the $L\leftarrow B$ transition.

From the work of Letzelter *et al.*,[3] which is reproduced by Eidelsberg *et al.*,[8] it is known that the L state predissociates and that the lifetime is of the order of 100 ps. In the present work the lifetime is deduced from the widths of the transitions observed. The observed line profiles are therefore fit to a Lorentzian line profile. Since the homo-

TABLE IV. Molecular constants (cm^{-1}) and predissociation rates (s^{-1}) for the $L\,^1\Pi(v=0)$ state of CO.

	This work	References 8 and 10	Reference 12	References 13 and 14
B'_e	1.981 73(53)	1.9796(18)		1.998(14)
B'_f	1.959 72(36)		[a]	1.959 68(24)
D'	6.7×10^{-6} [a]	$9(3)\times10^{-6}$	[a]	$6.7(1)\times10^{-6}$
q_π	0.022 01(40)		[a]	0.0213(12)
ν_{00}	16 355.6420(30)			16 355.660(12)
T_0	10 3271.7921(41)	10 3271.9(1)	10 3271.87(2)	10 3271.808(12)
Γ_{0f}	0.0097(7)			
Γ_{0e}	0.0101(4)			
α_e	0.006 35(10)			
k_{0f}	$1.83(13)\times10^9$	1×10^{10}	$<3\times10^{10}$	
k_{0e}	$1.91(7)\times10^9$	1×10^{10}	[b]	
k_{α_e}	$1.20(2)\times10^9$		[b]	

[a]Kept fixed at the value obtained by Sekine (Ref. 14).
[b]In a recent study on the L state a J-dependent linewidth was observed for the Π^+ levels (Ref. 37).

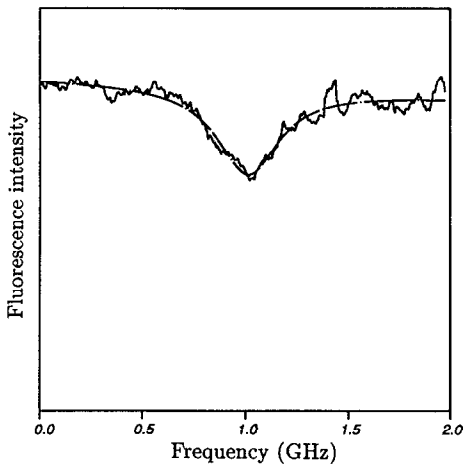

FIG. 6. Observed line profile of the $Q(2)\,L^1\Pi(v'=0) \leftarrow B^1\Sigma^+(v''=0)$ transition (solid line) and calculated Lorentzian line profile with a linewidth (FWHM) of 0.0097 cm^{-1} (dashed line).

geneous line broadening caused by the predissociation is much larger than the bandwidth of the probe laser, no large error is introduced by fitting the observed transition to a Lorentzian line profile. The linewidths obtained are then corrected for saturation broadening as described in Sec. III. Figure 6 shows the observed $Q(2)$ transition together with the fitted line profile. Although the line profile observed is quite noisy the linewidth can still be determined with an accuracy of 10%. As can be seen from Table III the linewidth depends strongly on the rotational level observed. When the linewidths are plotted as a function of $J(J+1)$, as is done in Fig. 7, it can be seen that for the $\Pi^-(f)$ component the linewidth is independent of J, whereas for the $\Pi^+(e)$ component the linewidth is almost proportional to $J(J+1)$. The observed linewidths for the $\Pi^+(e)$ component are therefore fit to the following expression for the linewidth:

$$\Gamma_e=\Gamma_{0e}+\alpha_e J(J+1). \tag{11}$$

The observed linewidths are very well described by this expression except for $J=4$. The calculated linewidth of 0.138 cm^{-1} for this level is considerably smaller than the observed width of 0.181(20) cm^{-1}. Probably this level is locally perturbed, like the $J=7$ level of the Π^- (f) component, by a crossing with a (pre)dissociating state. The predissociation rate for the Π^+ (e) component is now best described by

$$k_{pe}=k_{0e}+k_{\alpha_e}J(J+1), \tag{12}$$

with $k_{0e}=2\pi\Gamma_{0e}$ and $k_{\alpha_e}=2\pi\alpha_e$. The resulting values from the least squares fit for the parameters describing the linewidth and predissociation rate are given in Table IV. The obtained lifetimes for the Π^- (f) levels are nearly an order of magnitude larger than the values of Eidelsberg *et al.*[8]

C. $L'(3d\pi)^1\Pi(v=1)$ state

Since the $L'\ ^1\Pi(v=1)$ state and the $L\ ^1\Pi(v=0)$ state are very close in energy the two bands overlap when observed by low resolution spectroscopy. In the present experiment where we start from one rotational level in the B state these two states can easily be separated. The B state is populated by the PDA system whereafter the L' state is probed by the pulsed dye laser. Figure 8 shows a scan of the dye laser after populating the $J=2$ level in the B state. The intensities of the different transitions directly reflect the Hönl–London factors for these transitions. The transitions frequencies together with their assignments are listed in Table V. The observed frequencies have been fit to a $^1\Pi \leftarrow {}^1\Sigma^+$ transition. The resulting molecular constants are listed in Table VI. For comparison the molecular constants found by Eidelsberg,[8,10] Levelt,[12] and Sekine[15] have been included in Table VI.

It is well known that the L' state strongly predissociates.[3,8,12] This is confirmed by our results. The observed linewidth which is J independent, this in contrast to the L state, is 1.22 ± 0.06 cm^{-1}. This value for the linewidth corresponds to a predissociation rate of 2.26 ± 0.11

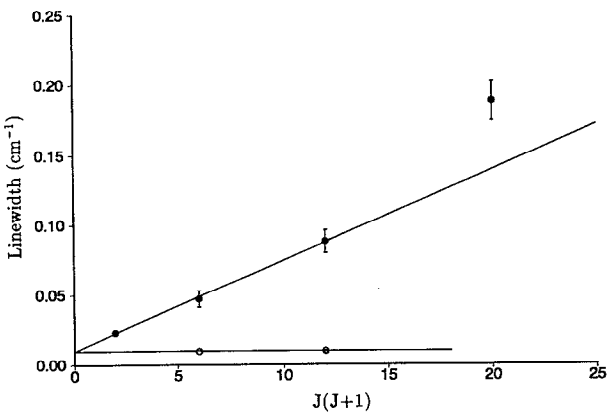

FIG. 7. Linewidths observed (cm^{-1}) for the Π^- (f) (open dots) and the Π^+ (e) levels (solid dots) of the $L\ ^1\Pi(v=0)$ state as function of $J(J+1)$.

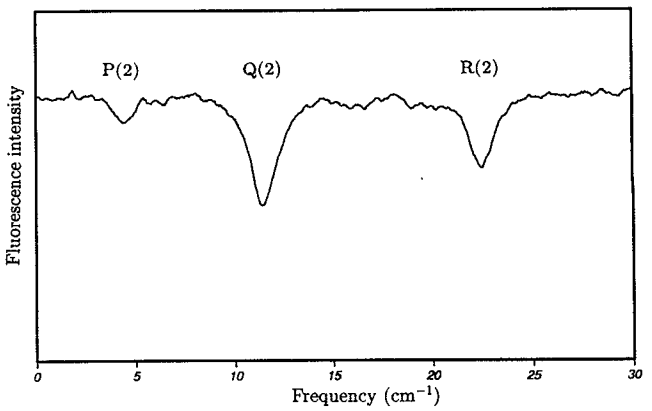

FIG. 8. The laser-depleted fluorescence dip spectrum of the $L'\ ^1\Pi(v'=1) \leftarrow B\ ^1\Sigma^+(v''=0)$ transition after populating the $J=2$ level in the B state.

TABLE V. Observed and calculated line positions and observed linewidths, all in cm^{-1}, of the $L'^1\Pi(v'=1) \leftarrow B^1\Sigma^+(v''=0)$ transition. The values given in parentheses are the relative errors for the measured line positions. The absolute uncertainty in the line positions is 0.5 cm^{-1}.

Transition	Obs. freq.	Obs.-calc.	Γ
$P(2)$	16 287.41(6)	0.01	1.13(9)
$P(3)$	16 282.86(6)	−0.04	1.27(14)
$Q(1)$	16 295.15(6)	0.01	1.27(9)
$Q(2)$	16 294.40(6)	0.01	1.26(9)
$Q(3)$	16 293.22(6)	0.05	1.24(14)
$R(0)$	16 299.10(6)	−0.01	1.21(7)
$R(1)$	16 302.38(6)	−0.01	1.21(6)
$R(2)$	16 305.35(6)	0.01	1.24(8)
$R(3)$	16 308.02(6)	0.01	1.11(17)

$\times 10^{11}$ s^{-1} and a lifetime of 4.42 ± 0.22 ps, a value in agreement with the aforementioned experiments.

D. $K(4p\sigma)^1\Sigma^+(v=0)$ state

The K state is the second member ($n=4$) of the $np\sigma$ Rydberg series converging to the electronic ground state of CO^+. It has been studied by several different techniques. There is, however, a rather large discrepancy in the B rotational constants found (see Table VIII).

The $K(v=0)$ state is measured with the same experimental setup as the $L(v=0)$ state. The observed line frequencies of the $K^1\Pi(v=0) \leftarrow B^1\Pi(v=0)$ transition together with their assignments are listed in Table VII. The observed line positions have been fit to a $^1\Sigma^+ \leftarrow {}^1\Sigma^+$ transition. The resulting molecular constants for the K state are listed in Table VIII. The value found for the B rotational constant agrees best with the value found by Eidelsberg.[8]

It is known that already the first member of the $np\pi$ Rydberg series, $E^1\Pi(v=0)$, predissociates. Moreover, the $K^1\Pi$ state is known to predissociate. Levelt *et al.*[12] have deduced from the the observed linewidths a predissociation rate of $(2.7 \pm 1.8) \times 10^{10}$ s^{-1} for this state. In the present experiment we found that the predissociation rate is independent of the rotational level and has a value of $(2.22 \pm 0.13) \times 10^{10}$ s^{-1}, corresponding to a lifetime of 45 ± 3 ps.

TABLE VI. Molecular constants (cm^{-1}), predissociation rate (s^{-1}), and lifetime (s) for the $L'^1\Pi(v=1)$ state.

	This work	References 8 and 10	Reference 12	Reference 16
B'_e	1.7931(15)	1.7966(23)	[a]	
B'_f	1.7603(13)			1.7535(48)
D'	1.0×10^{-5} [a]	$1.0(5) \times 10^{-5}$	[a]	$1.0(9) \times 10^{-5}$
q_π	0.0328(22)			
ν_{00}	16 295.5(5)			16 295.6(4)
T_0	103 211.6(5)	103 211.8(1)	103 211.88(5)	10 3211.8(4)
Γ	1.22(6)		1.4(5)	
k_p	$2.26(11) \times 10^{11}$		$2.7(9) \times 10^{11}$	
τ	$4.42(22) \times 10^{-12}$	3×10^{-12}	$3.7(13) \times 10^{-12}$	

[a]Kept fixed in the fit at the value obtained by Eidelsberg (Ref. 8).

TABLE VII. Observed and calculated line positions and linewidths (in cm^{-1}) of the $K^1\Sigma^+(v'=0) \leftarrow B^1\Sigma^+(v''=0)$ transition.

Transition	Obs. freq.	Obs.-calc.	Γ
$P(2)$	16 130.649(10)	−0.003	0.110(13)
$P(3)$	16 126.630(10)	0.003	0.122(12)
$R(2)$	16 149.810(10)	0.001	0.125(14)
$R(3)$	16 153.436(10)	−0.001	0.114(11)

E. $W(A^2\Pi)(3s\sigma)^1\Pi(v=0)$ state

The $W^1\Pi$ state is the first member of the $(1\pi)^3$ $ns\sigma$ Rydberg series converging to the first electronically excited state, $A^2\Pi$, in the CO^+ ion. The rotational and vibrational constants determined for this state are quite different from the constants found for Rydberg states converging to the ionic ground state and are close to the constants for the $A^2\Pi$ state in CO^+.

The $W(v=0)$ state has been measured with the same experimental setup as the L and the K state. The measured line positions, see Table IX, have been fit to a $^1\Pi \leftarrow {}^1\Sigma^+$ transition. The resulting molecular constants for the W state are listed in Table X. The Λ doubling parameter q_π found for this state is almost equal to zero, this in contrast to the other Rydberg states converging to the ionic ground state.

From the experiments of Levelt *et al.*[12] it is known that also the W state predissociates. They obtained in their experiments a J independent predissociation rate of $(3.6 \pm 1.9) \times 10^{10}$ s^{-1}. In the present experiment we find, however, a J-dependent linewidth, see Table X, resulting in a J-dependent predissociation rate. In Fig. 9 the observed linewidth is plotted as a function of $J(J+1)$. It can directly be seen that for the Π^+ (e) component the linewidth is proportional to $J(J+1)$, whereas for the Π^- (f) component the linewidth is J independent, just as is seen for the L state. The observed linewidths for the Π^+ component have been fit to Eq. (11). The resulting constants for the linewidths together with those for the predissociation rate are listed in Table X. These results differ considerably from the results of Levelt *et al.*[12] who obtained a J-independent predissociation for both Λ doublet components. The J dependence most probably was not observed due to the absence of high rotational (e) levels in their

TABLE VIII. Molecular constants (cm^{-1}) obtained for the $K^1\Sigma^+(v=0)$ state.

	This work	References 8 and 10	Reference 12	Reference 13
B'	1.916 53(22)	1.916 64(27)	1.9159(2)	1.900(2)
D'	5.85×10^{-5} [a]	$6.0(1) \times 10^{-5}$	$5.85(6) \times 10^{-5}$	5.3×10^{-5}
ν_{00}	16 138.5037(48)			16 138.08
T_0	103 054.6590(72)	103 054.57(2)	103 054.71(2)	103 054.23(8)
Γ	0.118(7)		0.14(10)	
k_p	$2.22(13) \times 10^{10}$		$2.7(18) \times 10^{10}$	
τ	$4.50(27) \times 10^{-11}$	1×10^{-10}	$3.7(25) \times 10^{-11}$	

[a]Kept fixed at the value of Levelt (Ref. 12).

TABLE IX. Observed and calculated line positions and observed linewidths, all in cm^{-1}, of the $W\,^1\Pi(v'=0) \leftarrow B\,^1\Sigma^+(v''=0)$ transition.

Transition	Obs. freq.	Obs.-calc.	Γ
$P(2)$	15 881.923(12)	−0.008	0.065(8)
$P(3)$	15 876.516(24)	0.007	0.122(9)
$Q(2)$	15 888.219(11)	0.009	0.055(7)
$Q(3)$	15 885.908(11)	−0.005	0.048(6)
$R(2)$	15 897.584(40)	0.003	0.202(14)
$R(3)$	15 898.388(64)	−0.005	0.325(35)

spectra of the W state, where the extra line broadening should become observable. The fact that the higher rotational levels are not observed already indicates that the predissociation for these levels is faster than for low rotational levels.

F. $W'\,^1\Pi(v=2)$ state

The $W'\,^1\Pi(v=2)$ state around 102 310 cm^{-1} has first been observed by Ogawa and Ogawa[38] in 1974. They were, however, not able to assign this band to a member of a Rydberg series. Later Hammond *et al.*[39] observed this state in a threshold electron spectroscopy study on CO, but they also couldn't assign this band. Recently Eidelsberg and Rostas[8] assigned this band as the $v=2$ level of the first member ($n=3$) of the $(A\,^2\Pi)ns\sigma\,^3\Pi$ Rydberg series converging to the first electronically excited state in CO^+. They based their result on the fact that the observed rotational and vibrational constants for this series are close to those of the $A\,^2\Pi$ state of the CO^+ ion. Furthermore, the observed intensity for the transition is very low as expected for a $^3\Pi \leftarrow {}^1\Sigma^+$ transition.

The $W'(v=2)$ state has been measured with the same experimental setup as the $L'(v=1)$ state. In order to probe higher rotational levels in the W' state the rotational temperature is increased to about 10 K by placing a skimmer between the nozzle and the detection zone. The observed line positions for the $W'(v'=2) \leftarrow B(v''=0)$ transition are listed in Table XI. In a first attempt the observed line positions have been fit to a $^3\Pi \leftarrow {}^1\Sigma^+$ transition. The Hamiltonian describing a $^3\Pi$ state is taken from Ref. 40. Only the P and R transitions observed could be fit within their experimental error to this transition. The Q transitions and especially the Q transitions of high J levels observed by Eidelsberg[9] could not be fit within their error to this type of transition. From the fit a spin–orbit coupling constant of $A=25$ cm^{-1} was obtained. For this value of A the Hunds case (a) wave functions describing the $^3\Pi$ state are almost completely mixed for $J=5$. This implies that already for relatively low J levels transitions to the three different states, $^3\Pi_0$, $^3\Pi_1$, and $^3\Pi_2$, become equally probable. These transitions are however not observed. It can therefore be concluded that the W' state is *not* a $^3\Pi$ state. As a consequence, this state cannot be assigned as a mem-

TABLE X. Molecular constants (cm^{-1}) and predissociation rates (s^{-1}) for the $W\,^1\Pi(v=0)$ state of CO.

	This work	References 8 and 10	Reference 12	Reference 15
B'_e	1.5650(17)	1.562 16(27)	1.5634(5)	1.5549(68)
B'_f	1.5668(13)			
D'	7.8×10^{-5} [a]	$7.8(9)\times10^{-5}$	$8.3(2)\times10^{-5}$	
q_π	0.002(2)			
ν_{00}	15 990.500(11)			15 891.6(6)
T_0	102 806.650(13)	102 807.0(2)	102 806.74(2)	102 807.8(6)
Γ_{0f}	0.051(4)		0.19(10)	
Γ_{0e}	0.037(2)		0.19(10)	
α_e	0.0140(3)			
k_{0f}	$9.6(8)\times10^9$	1×10^{10}	$3.6(19)\times10^{10}$	
k_{0e}	$7.0(4)\times10^9$	1×10^{10}	$3.6(19)\times10^{10}$	
k_{α_e}	$2.64(6)\times10^9$			

[a]Kept fixed at the value of Eidelsberg (Ref. 8).

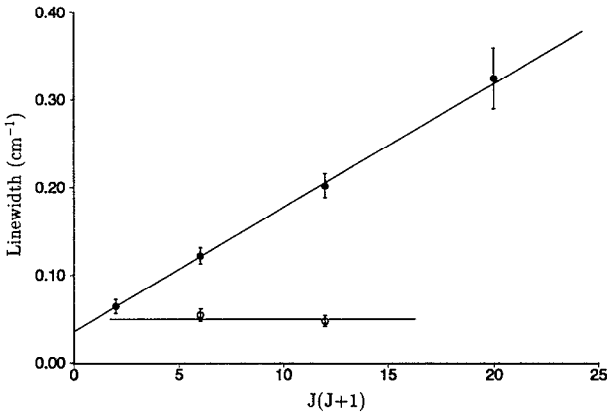

FIG. 9. Linewidths observed (cm^{-1}) for the Π^- (f) (open dots) and the Π^+ (e) levels (solid dots) of the $W\,^1\Pi(v=0)$ state as function of $J(J+1)$.

TABLE XI. Observed and calculated line positions and linewidths, in cm^{-1}, of the $W'\,^1\Pi(v'=2) \leftarrow B\,^1\Sigma^+(v''=0)$ transition. The values given in parentheses are the relative errors for the measured line positions. The absolute uncertainty in the line positions is 0.5 cm^{-1}.

Transition	Obs. freq.	Obs.-calc.	Γ
$P(2)$	15 387.31(10)	−0.01	2.04(15)
$P(3)$	15 381.48(10)	−0.01	2.30(17)
$P(4)$	15 374.86(10)	0.07	2.14(26)
$P(5)$	15 367.31(10)	0.04	2.08(44)
$P(6)$	15 358.94(10)	−0.03	1.89(52)
$Q(1)$	15 395.25(10)	−0.01	1.96(19)
$Q(2)$	15 393.66(10)	0.06	1.99(14)
$Q(3)$	15 391.13(10)	0.02	2.13(12)
$Q(4)$	15 387.71(10)	−0.08	2.44(28)
$Q(5)$	15 383.56(10)	−0.08	2.32(42)
$Q(6)$	15 378.74(10)	0.08	2.18(28)
$R(0)$	15 399.00(10)	−0.01	2.04(17)
$R(1)$	15 400.96(10)	−0.01	2.21(16)
$R(2)$	15 402.13(10)	0.07	2.13(19)
$R(3)$	15 402.37(10)	0.04	2.04(24)
$R(4)$	15 401.79(10)	−0.03	2.24(28)
$R(5)$	15 400.47(10)	−0.05	2.34(18)
$R(6)$	15 398.48(10)	0.03	2.04(50)

TABLE XII. Molecular constants (cm^{-1}), predissociation rate (s^{-1}), and lifetime (s) for the $W'^1\Pi(v=2)$ state.

	This work	References 8 and 10
B_e	1.532 81(63)	1.5365(36)
B_f	1.5417(24)	
D'	$0.8(7)\times10^{-5}$	$1.2(2)\times10^{-5}$
q_π	0.0111(27)	
ν_{00}	15 392.5(5)	
T_0	102 312.3(4)	102 311.0(2)
B_{Σ^+}	1.9[a]	
η	0.60(5)	
Δ	16(5)	
Γ	2.14(14)	
k_p	$3.86(21)\times10^{11}$	
τ	$2.59(14)\times10^{-12}$	1×10^{-11}

[a]Kept fixed in the least squares fit.

ber of the $(A\ ^2\Pi)\ ns\sigma\ ^3\Pi$ Rydberg series. Since it cannot be assigned as a member of any other Rydberg series it is most probably a valence state.

Since it is clear from combination differences that only the Π^+ (e) Λ doublet components are perturbed an interaction with a $^1\Sigma^+$ state is the most probable. The energy levels for the Π^- (f) components are then given by

$$\nu_{\Pi^-}=\nu_0+B'_fJ(J+1)+D'J(J+1). \tag{13}$$

The energy levels for the $\Pi^+(e)$ components are obtained by diagonalization of the matrix describing the interaction between a Π^+ and a Σ^+ state.[41] On the $|^1\Pi^+\rangle$, $|^1\Sigma^+\rangle$ basis this matrix is given by

$$\begin{pmatrix} \nu_0+B'_eJ(J+1)+D'J(J+1) & 2\eta\sqrt{J(J+1)} \\ 2\eta\sqrt{J(J+1)} & \nu_0+\Delta+B_{\Sigma^+}J(J+1) \end{pmatrix}. \tag{14}$$

Here B'_e and B_{Σ^+} are the rotational constants of the $^1\Pi^+$ and $^1\Sigma^+$ state, respectively, Δ is the energy difference and η the interaction strength between the two states. The transitions observed in the present experiment together with the transitions observed by Eidelsberg *et al.*[9] have been fit to these expressions. Since only transitions to the $^1\Pi$ state are observed not all the constants for the $^1\Sigma^+$ state can be determined. The parameter B_{Σ^+} has therefore been fixed at 1.9 cm^{-1}, a value common for Rydberg states converging to the ground state of the ion. All the observed line positions could be fit within their experimental error to this type of transition. The resulting molecular constants are listed in Table XII. As can be seen from Table XII the perturbing $^1\Sigma^+$ state is very close in energy, 16 cm^{-1}, to the $W'\ ^1\Pi(v=2)$ state. The mixing between the two states is small, less than 5%, even for high J levels and, as a consequence, the transitions to the $^1\Sigma^+$ state are too weak to be observed in the present experiment.

The linewidths observed for the $W'(v=2)$ state are independent of the rotational level and amount to 2.14 ±0.14 cm^{-1}. The corresponding predissociation rate and lifetime for this state are $(4.0\pm0.3)\times10^{11}$ s^{-1} and 2.5 ±0.2 ps, respectively.

V. DISCUSSION

In the present experiment the term values, T_0, for three of the Rydberg states have been determined within 0.01 cm^{-1}. In a first step the energy levels of the $B\ ^1\Sigma^+(v=0)$ state were accurately determined by calibrating the $B\ ^1\Sigma^+(v'=0)\leftarrow X\ ^1\Sigma^+(v''=0)$ transition to the Te_2 frequency standard.[25] In a second step the transitions from the B state to a Rydberg state were calibrated to the I_2 standard.[23,24] When our values obtained for the term values are compared with those obtained by Levelt *et al.*[12], who calibrated their transitions also to the I_2 standard, a systematic difference of 0.07 cm^{-1} is observed. Although this difference is within the experimental error of 0.13 cm^{-1} given by Levelt *et al.*, it is still significant. We therefore have checked carefully for possible lineshifts caused by saturation of the $B\leftarrow X$ transition. The transition could, however, not be saturated by the laser power used in the present experiment and consequently no lineshifts were observed. Since we have carefully avoided saturating the transitions to the Rydberg states no lineshifts were observed for these transitions. Furthermore lineshifts caused by the Autler–Townes effect can also be ruled out. Since there were no electric or magnetic fields present at the excitation region which can shift the energy levels we conclude that our values found for the term values of the Rydberg states are accurate within 0.01 cm^{-1}.

At an energy of about 103 000 cm^{-1} above the ground state of CO many electronic states can be expected which interact with each other, giving rise to perturbations in the observed spectra. In Sec. IV F it is concluded that the $W'\ ^1\Pi(v=2)$ state is perturbed by a state of $^1\Sigma^+$ symmetry. This $^1\Sigma^+$ state is most probably the $v=5$ level of the $C\ 3s\sigma\ ^1\Sigma^+$ state. The $v=5$ level of this state is calculate to lie within 50 cm^{-1} of the $W'\ ^1\Pi(v=2)$ state, using the values for ω_e and $\omega_e x_e$ given by Huber and Herzberg.[42] Direct transitions to the $v=5$ level of the C state are, however, too weak to be observed due to the poor Franck–Condon overlap with the ground state. Although the rotational B constant for the $C\ ^1\Sigma^+(v=5)$ could not be determined from the fit of the transitions to the $W'^1\Pi(v=2)$ the term value for the C state could be determined as well as the interaction strength between the two states. For the term value of the C state a value of $T_0=102\ 328\pm5$ cm^{-1} is found. The value of 0.6 cm^{-1} for the interaction strength η indicates that there is a rather good Franck–Condon overlap between the two interacting states. From the observed linewidths of the $W'\ ^1\Pi(v=2)$ state and calculated mixing between the two states limits can be given for the predissociation rate of the $C\ ^1\Sigma^+(v=5)$ state, i.e., $2\times10^{10}<k_p<1\times10^{12}$ s^{-1}.

Interactions of repulsive states with bound states such as the Rydberg states observed can cause predissociation of these bound states. The predissociation observed for the $L\ ^1\Pi(v=0)$, $K\ ^1\Sigma^+(v=0)$, and $W\ ^1\Pi(v=0)$ states is most probably caused by the interaction of these states with a repulsive state of $^1\Sigma^+$ symmetry. The interaction matrix element describing the interaction between $^1\Pi^+$ and $^1\Sigma^+$ states is proportional to $\sqrt{J(J+1)}$. This gives rise to a

$J(J+1)$ dependent predissociation rate for the $^1\Pi^+$ (e) levels as has been observed for the $L\,^1\Pi(v=0)$ state and the $W\,^1\Pi(v=0)$ state. Since there is no interaction between a $^1\Sigma^+$ and a $^1\Pi^-$ state possible the $^1\Pi^-$ state will not predissociate via the $^1\Sigma^+$ state. The linewidths observed for the Π^- (f) levels indicate, however, that these states also predissociate, probably due to weak interactions with dissociating states of other symmetry. The J-independent linewidth, Γ_{0e} found for the Π^+ (e) levels and the linewidths found for the Π^- (f) levels of the $L\,^1\Pi(v=0)$ correspond to a lifetime of 0.55 ± 0.03 ns. It can well be that this lifetime is solely determined by the radiative lifetime of the L state. A similar value for the radiative lifetime is found for the $C\,^1\Sigma^+(v=0)$ state.[43] The experiments of Letzelter *et al.*[3] on the fluorescence yield of the L state seem to indicate, however, that the observed lifetime is largely determined by predissociation. The results from these experiments have to be interpreted with some caution since the fluorescence yield is determined after excitation to several rotational levels in the L state with a broadband light source.

The predissociation observed for the $K\,^1\Sigma^+(v=0)$ is most probably caused by the same $^1\Sigma^+$ state responsible for the predissociation in the L and W state. The interaction between the two $^1\Sigma^+$ states is J independent and as a result the predissociation in the K state will not depend on the rotational quantum number, as has been observed.

The $^1\Sigma^+$ state which is responsible for the predissociation in these states can on energetic grounds only correlate to the ground state atoms C (^3P) and O (^3P). Only two $^1\Sigma^+$ states are expected to correlate to the ground states atoms, i.e., the $X\,^1\Sigma^+$ ground state and the $D'^1\Sigma^+$ valence state. The D' state which has only recently observed by Wolk and Rich[44] is very weakly bound at a relatively large internuclear distance. Recent calculation performed by Tchang–Brillet *et al.*[45] on the $D'\,^1\Sigma^+$ and $B\,^1\Sigma^+$ states show that the predissociation observed in the B state is caused by the interaction of the D' state with the B state. The predissociation observed for the Rydberg states $L\,^1\Pi$, $K\,^1\Sigma^+$, and $W\,^1\Pi$ is most probably also caused by an interaction of these states with the the D' valence state, whose repulsive part of the potential is expected to cross the potential of Rydberg states at the outer turning points.

The predissociation rates found for the $L'\,^1\Pi(v=1)$ and $W'\,^1\Pi(v=2)$ are much larger than those found for the $L\,^1\Pi(v=0)$, $K^1\Sigma^+(v=0)$, and $W\,^1\Pi(v=0)$ states. In contrast to these states the L' and the W' state show no J dependence of the predissociation rate. The perturbing state causing this strong predissociation can therefore not be the $^1\Sigma^+$ state which is responsible for the predissociation in the L, K, and W state nor can it be a state of $^1\Sigma^-$ or $^1\Delta$ symmetry which would also yield J-dependent predissociation rates. It has to be concluded that the perturbing state has $^1\Pi$ or $^3\Pi$ symmetry. The difference in interaction strength between the L' and W' and the L, K, and W states with the perturbing Π state is most probably due to a difference in Franck–Condon overlap between the wave functions of the interacting states. Since it is not clear whether the perturbing state has $^1\Pi$ or $^3\Pi$ symmetry it is not possible to identify the perturbing state. It can, however, very well be that this state is the same state which is responsible for the observed predissociation in the $E\,^1\Pi(v=0)$ state.[3,22]

VI. SUMMARY

In a 2+1 double resonance experiment on CO, where the $B\,^1\Sigma^+$ state is used as intermediate state, five Rydberg states around 103 000 cm^{-1} have been studied. Accurate molecular constants have been obtained. From the observed $W'(v=2)\leftarrow B\,^1\Sigma^+(v=0)$ transition it is concluded that the $W'(v=2)$ state is a $^1\Pi$ state and that it is perturbed by the $C\,^1\Sigma^+(v=5)$ state. From the observed linewidths predissociation rates for the Rydberg states could be determined. For the first time a clear J and e/f dependence for the predissociation rates could be observed. From the observed J dependence of the predissociation rates one of the perturbing states has been identified as the $D'\,^1\Sigma^+$ state.

ACKNOWLEDGMENTS

The authors wish to thank Dr. Giel Berden for his help with the data acquisition program and Dr. Gerard Meijer and Professor D. H. Parker for fruitful discussions and valuable suggestions. Professor R. W. Field is gratefully acknowledged for his suggestions on the interpretations of the observed predissociation rates. This research was made possible by the financial support of the Dutch Organization for Fundamental Research of Matter (FOM).

[1] E. F. van Dishoek and J. H. Black, in *Physical Processes in Interstellar Clouds*, edited by G. Morfill and M. S. Scholer (Reidel, Dordrecht, 1987), p. 241.
[2] E. F. van Dishoek and J. H. Black, Astrophys. J. **334**, 771 (1988).
[3] C. Letzelter, M. Eidelsberg, F. Rostas, J. Breton, and B. Thieblemont, Chem. Phys. Lett. **114**, 273 (1987).
[4] G. Stark, K. Yoshino, P. L. Smith, K. Ito, and W. H. Parkinson, Astrophys. J. **369**, 574 (1991).
[5] G. Stark, K. Yoshino, P. L. Smith, K. Ito, and W. H. Parkinson, Astrophys. J. **395**, 705 (1992).
[6] G. Stark, K. Yoshino, P. L. Smith, J. R. Esmond, K. Ito, and H. M. Stevens, Astrophys. J. (to be published).
[7] M. Eidelsberg, J. Y. Roncin, A. Le Floch, F. Launay, C. Letzelter, and J. Rostas, J. Mol. Spectrosc. **121**, 309 (1987).
[8] M. Eidelsberg and F. Rostas, Astron. Astrophys. **235**, 472 (1990).
[9] M. Eidelsberg, J. J. Benayoun, Y. Viala, and F. Rostas, Astron. Astrophys. Suppl. Ser. **90**, 231 (1990).
[10] M. Eidelsberg, J. J. Benayoun, Y. Viala, F. Rostas, P. L Smith, K. Yoshino, G. Stark, and A. Shettle, Astron. Astrophys. (to be published).
[11] P. F. Levelt, W. Ubachs, and W. Hogervorst, J. Phys. II France **2**, 801 (1992).
[12] P. F. Levelt, W. Ubachs, and W. Hogervorst, J. Chem. Phys. **97**, 7160 (1992).
[13] T. Masaki, Y. Adachi, and C. Hirose, Chem. Phys. Lett. **139**, 62 (1987).
[14] S. Sekine, T. Masaki, Y. Adachi, and C. Hirose, J. Chem. Phys. **89**, 3951 (1988).
[15] S. Sekine, Y. Adachi, and C. Hirose, J. Chem. Phys. **90**, 5346 (1989).
[16] S. Sekine, S. Iwata, and C. Hirose, Chem. Phys. Lett. **180**, 173 (1991).
[17] M. A. Hines, H. A. Michelsen, and R. N. Zare, J. Chem. Phys. **93**, 8557 (1990).

[18] N. Hosoi, T. Ebata, and M. Ito, J. Phys. Chem. **95**, 4182 (1991).
[19] T. Ebata, N. Hosoi, and M. Ito, J. Chem. Phys. **97**, 3920 (1992).
[20] K. Tsukiyama, M. Momose, M. Tsukakoshi, and T. Kasuya, Opt. Commun. **79**, 88 (1990).
[21] F. Merkt and T. P. Softley, Mol. Phys. **72**, 787 (1991).
[22] P. Klopotek and C. R. Vidal, Opt. Soc. Am. **2**, 869 (1985).
[23] S. Gerstenkorn and P. Luc, CNRS, Report, 1978.
[24] S. Gerstenkorn and P. Luc, Rev. Phys. Apl. **14**, 791 (1979).
[25] J. Cariou and P. Luc, CNRS, Report, 1980.
[26] M. A. Quesada, A. M. F. Lau, D. H. Parker, and D. W. Chandler, Phys. Rev. A **36**, 4107 (1987).
[27] S. N. Dobryakov and Y. S. Lebedev, Sov. Phys. Docl. **13**, 873 (1969).
[28] R. Loudon, *The Quantum Theory of Light* (Clarendon, Oxford, 1973).
[29] G. R. Cook, P. H. Metzger, and M. Ogawa, Can. J. Phys. **43**, 1706 (1965).
[30] Tilford and Vanderslice, J. Mol. Spectrosc. **26**, 419 (1968).
[31] Schmid and Gerö, Z. Phys. **93**, 656 (1935).
[32] G. W. Loge, J. J. Tiee, and F. B. Wampler, J. Chem. Phys. **79**, 196 (1983).
[33] P. J. H. Tjossem and K. C. Smyth, J. Chem. Phys. **91**, 2041 (1989).
[34] G. Guelachvili, D. de Villeneuve, R. Farrenq, W. Urban, and J. Verges, J. Mol. Spectrosc. **98**, 64 (1983).
[35] D. M. Cooper and S. R. Langhof, J. Chem. Phys. **74**, 1200 (1981).
[36] K. Kirby and D. L. Cooper, J. Chem. Phys. **90**, 4895 (1989).
[37] K. Eikema, W. Ubachs, and W. Hogervorst (private communication).
[38] S. Ogawa and M. Ogawa, J. Mol. Spec. **49**, 454 (1974).
[39] P. Hammond, G. C. King, J. Jureta, and F. H. Read, J. Phys. B **18**, 2057 (1985).
[40] M. Ebben, M. Drabbels, and J. J. ter Meulen, J. Chem. Phys. **95**, 2292 (1991).
[41] I. Kovacs, *Rotational Structure in the Spectra of Diatomic Molecules* (Adam Hilger, London, 1969).
[42] K. P. Huber and G. Herzberg, *Molecular Spectra and Molecular Structure. IV. Constants of Diatomic Molecules* (Van Nostrand-Reinhold, New York, 1979).
[43] M. Drabbels, W. L. Meerts, and J. J. ter Meulen, J. Chem. Phys. (to be published).
[44] G. L. Wolk and J. W. Rich, J. Chem. Phys. **79**, 12 (1983).
[45] W. Tchang-Brillet, P. S. Julienne, J. M. Robbe, C. Letzelter, and F. Rostas, J. Chem. Phys. **96**, 6735 (1992).